MOLECULAR AND CELLULAR BIOLOGY, Mar. 2006, p. 2317–2326 Vol. 26, No. 6
0270-7306/06/$08.00+0 doi:10.1128/MCB.26.6.2317–2326.2006

Generation and Characterization of *dickkopf3* Mutant Mice

Ivan del Barco Barrantes,[1]† Ana Montero-Pedrazuela,[2] Ana Guadaño-Ferraz,[2] Maria-Jesus Obregon,[2] Raquel Martinez de Mena,[2] Valérie Gailus-Durner,[3] Helmut Fuchs,[3] Tobias J. Franz,[4] Svetoslav Kalaydjiev,[4] Martina Klempt,[5] Sabine Hölter,[6] Birgit Rathkolb,[5] Claudia Reinhard,[7] Gabriella Morreale de Escobar,[2] Juan Bernal,[2] Dirk H. Busch,[4] Wolfgang Wurst,[6] Eckhard Wolf,[5] Holger Schulz,[7] Svetlana Shtrom,[8] Erich Greiner,[9] Martin Hrabé de Angelis,[3] Heiner Westphal,[8] and Christof Niehrs[1]*

Division of Molecular Embryology[1] and Molecular Biology of the Cell I,[9] Deutsches Krebsforschungszentrum, Im Neuenheimer Feld 280, D-69120 Heidelberg, Germany; Department of Molecular Endocrinology, Instituto de Investigaciones Biomédicas Alberto Sols, Consejo Superior de Investigaciones Científicas, Universidad Autónoma de Madrid, Arturo Duperier 4, E-28029 Madrid, Spain[2]; Institute of Experimental Genetics,[3] Institute of Developmental Genetics,[6] and Institute for Inhalation Biology,[7] GSF-National Research Center for Environment and Health, Ingolstaedter Landstr. 1, D-85758 Neuherberg, Germany; Institute for Medical Microbiology, Immunology, and Hygiene, Technical University of Munich, Trogerstr. 9, D-81675 Munich, Germany[4]; Institute of Molecular Animal Breeding and Biotechnology, Gene Center, Ludwig Maximilian University of Munich, Feodor-Lynen-Strasse 25, 81377 Munich, Germany[5]; and National Institutes of Health, 9000 Rockville Pike, Bethesda, Maryland 20892-2790[8]

Received 6 October 2005/Returned for modification 19 November 2005/Accepted 21 December 2005

***dickkopf* (*dkk*) genes encode a small family of secreted Wnt antagonists, except for *dkk3*, which is divergent and whose function is poorly understood. Here, we describe the generation and characterization of *dkk3* mutant mice. *dkk3*-deficient mice are viable and fertile. Phenotypic analysis shows no major alterations in organ morphology, physiology, and most clinical chemistry parameters. Since Dkk3 was proposed to function as thyroid hormone binding protein, we have analyzed deiodinase activities, as well as thyroid hormone levels. Mutant mice are euthyroid, and the data do not support a relationship of *dkk3* with thyroid hormone metabolism. Altered phenotypes in *dkk3* mutant mice were observed in the frequency of NK cells, immunoglobulin M, hemoglobin, and hematocrit levels, as well as lung ventilation. Furthermore, *dkk3*-deficient mice display hyperactivity.**

The Dickkopf family of secreted proteins consists of four members, which share two conserved cysteine-rich domains (12, 24). The hallmark of Dkk proteins is that they function as Wnt antagonists or agonists by binding to and inhibiting or activating the Wnt coreceptor LRP6 (1, 31, 45). They show regionalized expression during vertebrate embryogenesis (5, 10, 13, 18, 20, 33, 46). Dkk1 is the best-characterized member of the family. It acts as an embryonic head inducer, and when overexpressed it will induce extra heads in *Xenopus* and zebra fish (6, 12, 18, 22, 36, 46). *dkk1* mutant mice are embryonic lethal, and embryos lack anterior head structure and display fused digits (36). *dkk2* mouse mutants are viable but show bone defects (28). Little is known about the biological role of *dkk4*.

By a number of criteria, *dkk3* appears as a divergent member of the *dkk* family. (i) By DNA sequence similarity, vertebrate *dkk1*, *-2*, and *-4* are more related to each other than they are to *dkk3* (12). (ii) Hydra has two *dkk* genes, one related to vertebrate *dkk1*, *-2*, and *-4* (16) and one related to vertebrate *dkk3* (9). This suggests an ancient phylogenetic separation between these family members, where *dkk1*, *-2*, and *-4* but not *dkk3* arose by gene duplication from an ancestral *dkk* (16). (iii) Soggy is a protein of unknown function with sequence similarity to *dkk3* but not to other *dkk* genes (24). The similarity is most pronounced outside the two conserved Dkk cysteine-rich domains, raising the possibility that the gene arose from an ancestral *dkk3* precursor. (iv) Unlike Dkk1, -2, and -4, Dkk3 does not act as a Wnt modulator (24, 29, 55). While all other tested Dkk proteins bind to and modulate the Wnt receptor LRP6, as well as the Dkk coreceptor Kremen, Dkk3 has no affinity to these transmembrane proteins (7, 30, 32, 33), and no other proteins are known to interact with it.

Like other *dkk* members, *dkk3* is expressed during vertebrate development in suggestive patterns in many organs (7, 33). Prominent expression of *dkk3* is observed in the brain and in fibroblasts of adult rodents (17, 24, 34, 37, 56) and in the human adrenal cortex (50). Dkk3 has been proposed to act as a tumor suppressor, as it is downregulated in a number of tumor cells and since *dkk3* overexpression suppresses cell growth (19, 25, 37, 52, 53). Hence, *dkk3* is also known as *REIC* (for *r*educed *e*xpression in *i*mmortalized *c*ells) (52). While hy-

* Corresponding author. Mailing address: Division of Molecular Embryology, Deutsches Krebsforschungszentrum, Im Neuenheimer Feld 280, D-69120 Heidelberg, Germany. Phone: 49-6221-42-4690. Fax: 49-6221-42-4692. E-mail: niehrs@dkfz-Heidelberg.de.

† Present address: Cell Signalling Group, Centro Nacional de Investigaciones Oncologicas (CNIO), Melchor Fernández Almagro 3, E-28029 Madrid, Spain.

permethylation of human *dkk3* correlates with certain cancers (23, 43), the physiological relevance of altered *dkk3* expression in tumors and its potential growth inhibitory effect are unknown.

A cDNA encoding an N-terminally truncated Dkk3 lacking the signal peptide was cloned and characterized as a presumed substrate binding subunit, "p29," of the type II iodothyronine 5′-deiodinase (D2) in rat (26). The evidence for a role for p29 in thyroid hormone metabolism rests on the findings that p29 can be cross-linked to a thyroid hormone affinity label and that transfection of p29, directly or indirectly, enhances D2 activity in cultured astrocytes (26). Deiodinases play an important role in the local availability of brain, brown adipose tissue (BAT), and pituitary 3,5,3′-triiodothyronine (T3), which is converted from thyroxine (T4) by deiodination (2). This is different from other organs, which derive their T3 directly from plasma. All deiodinases (D1, D2, and D3) thus far characterized are selenoproteins that catalyze the removal of iodine atoms from iodoamino acids (4). The claim that an N-terminally truncated rat Dkk3 (p29) may be involved in D2 activity is controversial because (i) of the seleno nature of all other cloned deiodinases that act without substrate binding subunits and (ii) there is poor correlation between *dkk3*/*p29* and the D2 expression patterns in rat brain (34).

In summary, despite numerous studies of *dkk3*, its biological role and biochemical function remain largely elusive. We have therefore generated *dkk3* mutant mice by targeted disruption of the gene. Here, we present a first phenotypic characterization of these mice. Our data indicate that the gene is not essential for embryogenesis and viability, and the data do not support a role for Dkk3 in thyroid hormone metabolism. Instead, initial phenotyping indicates altered phenotypes in hematological and immunology parameters, lung ventilation, and behavior in *dkk3* mutant mice.

MATERIALS AND METHODS

Generation of *dkk3* mutant mice. The targeting vector was derived from a 129/SVJ bacterial artificial chromosome clone that includes exon 2 from the *dkk3* gene. The construct, which replaced most of exon 2, consisted of an in-frame-cloned *lacZ* cassette, followed by a *loxP*-flanked neomycin resistance (*neo*) cassette, a 4-kb 5′ homology arm, and a 4.5-kb 3′ homology arm. The A subunit of diphtheria toxin was used as a counterselection marker (Fig. 1A). 129/SVJ embryonic stem (ES) cells were electroporated, and correct recombination events were verified by Southern blot analysis of genomic DNA digested with BamHI, using both internal and external probes (Fig. 1B and C). Injection of two independent positives clones generated chimeras, which transmitted the recombinant locus. No difference was evident between the two lines, and we used one for further study. Genotyping of *dkk3*$^{-/-}$ mice was performed by a triplex PCR on genomic tail DNA using oligonucleotides p1 (5′-GATAGCTTTCCGGGACACAC-3′), p2 (5′-TCCATCAGCTCCTCCACCTCT-3′), and p3 (5′-TAAGTTGGGTAACGCCAGGGT-3′) (Fig. 1A and B) to produce 220-bp and 199-bp bands from the wild-type (WT) and targeted allele, respectively (Fig. 1D). *dkk3* mutant mice were maintained in a C57BL/6 background. A group of 60 Dkk3 knockout animals, 30 males and 30 females, were observed during 12 months and compared to wild-type animals. No increase in mortality and no spontaneous tumor formation were observed with the Dkk3 knockout mice.

German Mouse Clinic (GMC) screen. General set up of the screen, husbandry, and multiparameter analysis were as previously described (11) and will be described in detail elsewhere.

Behavior screen. Mice were analyzed with the behavior screen at the age of 9 weeks (after 2 weeks of acclimatization in the module). Three days before being tested, an object (a metal cube) was placed into the home cage and removed 1 day before testing. The modified hole board test was carried out by standardized procedures as described previously (40, 41). For each trial (5-min observation time), an unfamiliar object (a blue plastic tube lid, similar in size to the metal cube) and the familiar object (a metal cube) were placed into the test arena with a distance of 2 cm between them. Manually recorded behavioral data were analyzed using Observer 4.1 software (Noldus, Wageningen, The Netherlands), the animal's track was videotaped, and its locomotor path was analyzed with a video tracking system (Ethovision 2.3, Noldus, Wageningen, The Netherlands). Data were statistically analyzed with SPSS software (SPSS, Inc., Chicago, Ill.). The chosen level of significance was a P value of <0.05.

Clinical-chemical and hematological screen. For the hematological investigations, 50 μl of blood per 12-week-old mouse was collected in an EDTA-coated tube (catalogue no. 078035; KABE) by puncturing the retro-orbital sinus with a nonheparinized glass capillary (0.8 mm in diameter, catalogue no. 1.28.13.1.2; Laborteam K&K, Munich, Germany) under ether anesthesia. The sample was immediately inverted several times to ensure a homogenous mixture of blood and anticoagulant and used for automated analysis with a blood analyzer, which was carefully validated for the analysis of mouse blood (ABC-Blutbild analyzer; Scil Animal Care Company GmbH, Viernheim, Germany). The influence of gender and genotype were tested by applying a two-way analysis of variance (variance equal) or general linear model (variance unequal). In the case of a significant influence of genotype on the parameter investigated, the significance of the mean differences within each sex was evaluated by the Student t test.

Lung function screen. When mice were 14 weeks old, whole-body plethysmography (8) was applied to measure spontaneous breathing patterns of unrestrained animals (51) at different levels of activity. Automated data analysis provided tidal volumes (TV), respiratory rates (f), minute ventilation (MV), inspiratory and expiratory times (Ti, Te), and peak inspiratory and peak expiratory flow rates (PIF and PEF) at 10-s intervals. Mean inspiratory and expiratory flow rates (MEF and MIF) were calculated from the ratio of tidal volume and the respective time interval. The fraction of inspiration (Ti/TT) was determined from the ratio of inspiratory time (Ti) to total time required for the breathing cycle (TT). Specific tidal volumes and minute ventilations (sTV and sMV) were calculated by relating the absolute values to the body weight of the animal. Breathing was analyzed for the above-mentioned parameters during phases of activity and rest. Statistical analyses were performed with a commercially available statistics package (Statgraphics; Statistical Graphics Corporation, Rockville, MD). Differences between strains were evaluated by Student's t test. Statistical significance was assumed at a P value of <0.05. Data are presented as mean values ± standard error of the mean (SEM).

Immunology screen. Blood samples were taken from 12-week-old mice. Peripheral blood leukocytes were isolated from 500 μl blood by erythrocyte lysis with NH_4Cl (0.17 M)-Tris buffer (pH 7.45) directly in 96-well microtiter plates. After subsequent washing with fluorescence-activated cell sorter staining buffer (phosphate-buffered saline [PBS], 0.5% bovine serum albumin, 0.02% sodium azide, pH 7.45), peripheral blood leukocytes were incubated for 20 min with 1 μM ethidium monazide bromide (Molecular Probes, The Netherlands) and Fc block (clone 2.4G2; PharMingen, San Diego, Calif.). Ethidium monazide bromide bound to the DNA of dead cells was photo-cross-linked by brief light exposure. Cells were then stained with fluorescence-conjugated monoclonal antibodies (PharMingen). The following main cell populations were analyzed: B cells (CD19$^+$ clone 1D3), B1 B cells (CD19$^+$ CD5$^+$; clone 53-7.3), B2 B cells (CD19$^+$ CD5$^-$), T cells (CD3$^+$; clone 145-2C11), CD4$^+$ T cells (clone RM4-5), CD8$^+$ T cells (CD8β; clone H35-17.2), γ/δ T cells (clone GL3), granulocytes (Gr-1$^+$; clone RB6-8C5), and NK cells (CD49b$^+$; clone DX5). Data were acquired on a FACScalibur (Becton Dickinson, San Diego, Calif.) and were analyzed using FlowJo software (TreeStar Inc.). All samples were acquired until a total number of 25,000 cells were reached. The plasma levels of immunoglobulin M (IgM), IgG1, IgG2a, IgG2b, IgG3, and IgA were determined by standard sandwich enzyme-linked immunosorbent assays using goat anti-mouse immunoglobulin antibodies and alkaline phosphatase conjugates (SouthernBiotech, Birmingham, Ala.).

Animals and treatments for D2 studies. C57BL/6 animals were kept under temperature-controlled (22 ± 2°C) and light-controlled (12-h light and 12-h dark cycle; lights on at 0700 h) conditions and had free access to food and water. Animal care procedures were conducted in accordance with the guidelines set by European Community Council Directives (86/609/EEC).

For in situ hybridization studies, 11-day-old (P11) male wild-type and *dkk3* mutant mice were used. This postnatal day was chosen because it is comparable to the age at which the highest levels of *D2* activity and expression are found in rat brain (15, 21). For the determinations of deiodinase activities and thyroid hormones levels, four months-old mice were used from both wild-type and *dkk3* mutant mice. As we observed sex-related differences in these determinations with several tissues, groups of males and females of both groups were used (7 to 12 mice per group).

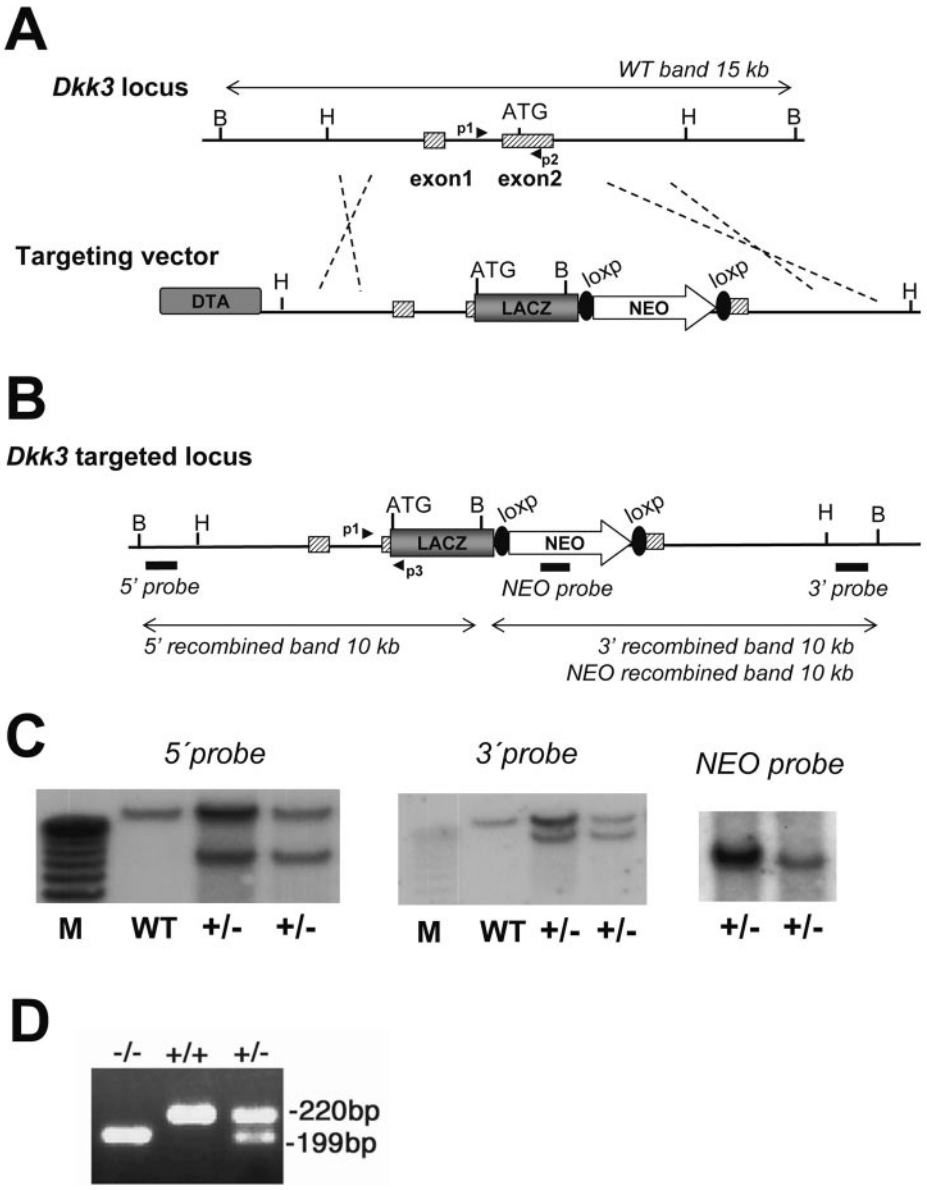

FIG. 1. Generation of *dkk3* mutant mice. (A) Schematic diagram of the *dkk3* locus and targeting construct. The construct contains 4 kb of the 5′and 3′ *dkk3* genomic sequence. A *lacZ* reporter gene followed by a floxed PGKNEO (NEO) selection marker replaces most of the coding sequence in exon 2. A counterselection cassette encoding the A subunit of diphtheria toxin (DTA) was inserted at the 5′ end of the vector. The wild-type band expected from a BamHI digestion is 15 kb. (B) Schematic diagram of the *dkk3* targeted allele. After homologous recombination in ES cells, the *lacZ* reporter gene is maintained in frame with the initial ATG. The probes and restriction enzymes are indicated, with the size of the resulting recombined restriction fragments. (C) Southern blot analysis after digestion with BamHI and hybridization with external 5′ and 3′ probes and internal NEO probe of two positive independent ES clones. (D) Triplex PCR of mouse genomic DNA from $dkk3^{-/-}$ mice (−/−), wild-type mice (+/+), and heterozygous mice (+/−). A single 199-bp fragment appears in the case of $dkk3^{-/-}$ mice, a single 220-bp fragment appears in the case of wild-type mice, and both fragments appear in the case of heterozygous mice. Abbreviations: H, HindIII; B, BamHI; M, marker.

cRNA probes. A *dkk3*-specific probe spanning nucleotides 287 to 640 (404 bp, encompassing exons 2 to 6) from the mouse cDNA sequence (NM_015814) (33) was used. A specific rat *p29* probe (nucleotides 1172 to 1499, 328 bp; AF245040) and specific *D2* probe (nucleotides 535 to 901, 366 bp; U53505) were used as previously described (15, 34). The sense and antisense riboprobes for in situ hybridization were synthesized with suitable RNA polymerase (SP6 or T7) in the presence of ^{35}S-labeled UTP (NEN Life Science Products) by in vitro transcription.

In situ hybridization histochemistry. Mice were fixed by transcardial perfusion with 4% paraformaldehyde–0.1 M phosphate buffer, pH 7.4. Cryoprotected brains were frozen in dry ice, and 25-μm-thick sections were obtained with a cryostat.

The detection of *p29*, *D2*, and *dkk-3* mRNAs with ^{35}S-labeled riboprobes was performed with free-floating sections according to protocols previously described in detail (3). Due to the floating procedure, there are structures such as the leptomeninges and choroid plexus that were not well preserved in all sections. Briefly, the sections were pretreated in different solutions for 10 min at room temperature; each section was permeabilized with 0.05% Triton X-100 in PBS, deproteinized with 0.2 N HCl, acetylated with 0.25% acetic anhydride in 0.1 M triethanolamine buffer (pH 8.0), postfixed in fixative, and washed in PBS. Hybridization was performed at 55°C for 16 h, with the ^{35}S-labeled riboprobe at 1.6×10^7 cpm/ml. The sections were mounted on coated slides, dehydrated, air

TABLE 1. Results of GMC behavior screen[a]

Parameter	Control (A)			Mutant (B)			A~B (*P* value)	
	Male (n = 11)	Female (n = 15)	*P* value	Male (n = 7)	Female (n = 15)	*P* value	Male	Female
Behavioral observation in the modified hole board test								
Line crossing (frequency)	76.82 ± 4.36	94.73 ± 5.33	NA	92.57 ± 6.65	114.20 ± 7.29	NA	NS	0.05
Rearings in box (frequency)	22.64 ± 1.82	31.40 ± 2.67	NA	25.43 ± 3.36	31.00 ± 2.97	NA	NS	NS
Hole exploration (frequency)	14.45 ± 2.45	6.00 ± 1.12	NA	11.71 ± 2.49	9.60 ± 1.60	NA	NS	NS
Board entry (frequency)	3.91 ± 1.07	1.80 ± 0.56	NA	4.29 ± 1.38	2.67 ± 0.65	NA	NS	NS
Board entry (latency)	155.43 ± 25.85	208.31 ± 23.46	NA	175.03 ± 35.64	193.08 ± 23.08	NA	NS	NS
Board entry (% total duration)	7.45 ± 1.57	2.30 ± 0.82	NA	6.04 ± 1.65	4.46 ± 1.06	NA	NS	NS
Rearing on board (frequency)	0.36 ± 0.28	0.27 ± 0.15	NA	0.43 ± 0.43	0.80 ± 0.24	NA	NS	NS
Grooming (frequency)	2.09 ± 0.49	1.80 ± 0.33	NA	1.71 ± 0.29	1.07 ± 0.25	NA	NS	NS
Video tracking of locomotor behavior								
Distance moved (cm)	2,173.83 ± 143.27	2,488.09 ± 115.50	NA	2,209.48 ± 194.12	2,958.40 ± 169.14	NA	NS	0.05
Mean velocity (cm/s)	14.68 ± 0.54	16.37 ± 0.53	NA	14.22 ± 1.17	17.96 ± 0.70	NA	NS	NS
Maximum velocity (cm/s)	60.04 ± 6.95	54.74 ± 2.48	NA	54.22 ± 6.61	64.09 ± 4.07	NA	NS	0.05
Turns (frequency)	1,331.18 ± 70.41	1,447.0 ± 49.24	NA	1,331.19 ± 108.57	1,626.50 ± 61.18	NA	NS	<0.05

[a] Data are from 9-week-old mice and are shown as means ± SEM. NA, not analyzed, NS, not significant.

dried, and exposed to Biomax MR film (Eastman Kodak, Rochester, NY) for 10 days for *dkk3* and *p29* expression analysis and for 2 weeks for *D2* studies. For cellular resolution, the sections were dipped in Hypercoat LM-1 photographic emulsion (Amersham Pharmacia Biotech), exposed for 20 to 40 days in the cold, developed, fixed, counterstained with Richardson's blue, and dehydrated, and coverslips were applied.

The autoradiographic films were scanned with a Coolscan II slide scanner (Nikon Corp., Tokyo, Japan) at a resolution of 400 pixels/inch and printed. Optical observations and photographs were carried otu with an Eclipse E400 microscope and Dn100 digital camera (both, Nikon Corp., Tokyo, Japan). For the identification of brain structures, the atlas of Paxinos and Franklin (42) was followed.

Deiodinase activities. Tissues were homogenized in buffer (0.32 M sucrose, 10 mM HEPES, 10 mM dithiothreitol [DTT; 1 mM DTT for liver and kidney], pH 7.0). Before each assay, ^{125}I-labeled T4 or ^{125}I-labeled reverse T3 (rT3) was purified from the iodide traces. The amount of iodide in the blanks was <0.5 to 1% of the total radioactivity. D2 activity was determined for tissue homogenates as previously described (39) using ^{125}I-labeled T4, 2 nM T4, 1 μM T3, 20 mM DTT, and 1 mM propylthiouracil. Results are expressed in femtomoles per hour per milligram of protein. Detection limits were 2 to 3 fmols/h · mg of protein. D2 activity was also assayed in the neocortex and cerebellum with ^{125}I-labeled rT3 as a substrate (2 nM); similar results were obtained (not shown). D1 activity in liver and kidney homogenates was assayed (44) using ^{125}I-labeled rT3, 400 nM rT3, and 2 mM DTT. Results are expressed in picomoles per hour per milligram of protein. Pituitary D1 and D2 activity was assayed with ^{125}I-labeled rT3, 2 nM rT3, and 20 mM DTT in the presence or absence of 1 mM propylthiouracil (for D2 and total deiodinase activity, respectively). Results are given in femtomoles per hour per milligram of protein.

T4 and T3 determination in tissues. Thyroid hormones were determined by radioimmunoassays (RIAs) after extraction and purification of plasma and tissues (35, 38). Frozen tissue samples were homogenized in methanol with tracer amounts of ^{131}I-labeled T4 and ^{125}I-labeled T3, added to each homogenate. The iodothyronines were extracted by chloroform-methanol (2:1), back extracted into an aqueous phase, and purified through Bio-Rad AG 1X2 resin columns. The purified iodothyronines were then evaporated to dryness and dissolved in RIA buffer. Each extract was counted to determine the recovery of the ^{131}I-labeled T4 and ^{125}I-labeled T3 in each sample. The samples are submitted to RIAs for the determination of T4 and T3, the limits of sensitivity being 2.5 pg T4 and 1.5 pg T3. Each sample was processed in duplicate at 2 dilutions. Concentrations were calculated using the amounts of T4 and T3 found in the RIAs, the individual recovery of the ^{131}I-labeled T4 and ^{125}I-labeled T3 added to each sample, and the weight of the tissue sample extracted.

High-specific-activity ^{131}I-labeled T4, ^{125}I-labeled T3, ^{125}I-labeled T4, and ^{125}I-labeled rT3 (3,000 μCi/μg) were synthesized in our laboratory as previously described (35) and used for the highly sensitive T4 and T3 RIAs as recovery tracers for plasma and tissue extractions and as substrates for D1 and D2 deiodinases.

Data are presented as mean values (±SEM). One-way analysis of variance was applied after ensuring homogeneity of variance by Bartlett's test. Statistically significant differences between mean values of different groups were then identified by the least-significant-difference method. All calculations were performed as previously described (49).

RESULTS AND DISCUSSION

Generation of *dkk3* mutant mice. A targeting vector was designed to constitutively disrupt *dkk3* exon 2, containing the signal sequence, by insertion of a *lacZ neo* cassette (Fig. 1). A homologous recombinant ES clone was generated and used to derive chimeras which gave rise to *dkk3*$^{+/-}$ pups. Intercrossing of these heterozygous mice produced homozygous *dkk3*$^{-/-}$ offspring, which were viable and fertile and obtained at the expected Mendelian ratio. *dkk3*$^{-/-}$ embryos and adults were examined by X-galactosidase staining but failed to produce any

TABLE 2. Results of the GMC hematological screen[a]

Hematological parameter	Control (A)			Mutant (B)			A~B (*P* value)	
	Male (n = 14)	Female (n = 14)	*P* value	Male	Female	*P* value	Male	Female
White blood cell count (10^3/μl)	8.57 ± 0.78	5.61 ± 0.46	<0.01	7.87 ± 0.42	6.65 ± 0.52	NS	NS	NS
Red blood cell count (10^6/μl)	10.26 ± 0.16	10.07 ± 0.19	NS	10.27 ± 0.16	10.30 ± 0.14	NS	NS	NS
Hemoglobin (g/dl)	14.96 ± 0.25	15.21 ± 0.27	NS	15.62 ± 0.24	16.01 ± 0.19	NS	NS	<0.05
Hematocrit (%)	46 ± 0.79	45 ± 0.83	NS	50 ± 0.98	50 ± 0.74	NS	<0.01	<0.001
Mean corpuscular volume (fl)	44.79 ± 0.24	45.07 ± 0.25	NS	48.73 ± 0.33	48.80 ± 0.24	NS	<0.001	<0.001
Mean corpuscular hemoglobin (pg)	14.52 ± 0.08	15.14 ± 0.08	<0.001	15.20 ± 0.09	15.57 ± 0.10	<0.02	<0.001	<0.01
Mean corpuscular hemoglobin concn (g/dl)	32.55 ± 0.12	33.56 ± 0.11	<0.001	31.20 ± 0.17	31.93 ± 0.18	<0.01	<0.001	<0.001
Platelet count (10^3/μl)	888 ± 37.81	654 ± 59.38	<0.01	854 ± 35.97	756 ± 32.82	NS	NS	NS

[a] Data are from 12-week-old mice and are shown as means ± SEM. NS, not significant.

TABLE 3. Results of GMC lung function screen[a]

Spontaneous breathing pattern during rest and activity	Control (A)			Mutant (B)			A~B (*P* value)	
	Male ($n = 5$)	Female ($n = 4$)	*P* value	Male ($n = 5$)	Female ($n = 5$)	*P* value	Male	Female
Rest								
Respiratory rate (f) (1/min)	348.0 ± 13.0	368.7 ± 21.4	NS	333.1 ± 10.1	376.0 ± 20.4	NS	NS	NS
Tidal volume (TV) (ml)	0.29 ± 0.01	0.29 ± 0.01	NS	0.26 ± 0.01	0.22 ± 0.01	NS	NS	<0.01
Specific tidal volume (sTV) (μl/g)	9.1 ± 0.6	11.9 ± 0.5	<0.02	8.6 ± 0.2	9.8 ± 0.6	NS	NS	<0.05
Minute ventilation (MV) (ml/min)	99.6 ± 3.6	104.6 ± 6.6	NS	83.3 ± 3.0	84.0 ± 6.0	NS	<0.01	NS
Specific minute ventilation (sMV) (ml/g)	3.1 ± 0.2	4.3 ± 0.3	<0.02	2.8 ± 0.1	3.6 ± 0.4	NS	NS	NS
Inspiratory time (Ti) (ms)	64.5 ± 2.8	53.3 ± 3.1	<0.05	61.7 ± 3.0	50.6 ± 1.8	<0.02	NS	NS
Expiratory time (Te) (ms)	108.9 ± 4.5	110.9 ± 5.9	NS	119.0 ± 2.0	110.9 ± 7.0	NS	NS	NS
Fraction of respiration (Ti/TT)	0.37 ± 0.01	0.32 ± 0.01	<0.01	0.34 ± 0.01	0.31 ± 0.01	NS	NS	NS
Peak inspiratory rate (PIF) (ml/s)	7.6 ± 0.5	9.4 ± 0.5	NS	7.6 ± 0.3	8.2 ± 0.5	NS	NS	NS
Peak expiratory rate (PEF) (ml/s)	6.6 ± 0.4	6.5 ± 0.6	NS	6.2 ± 0.5	5.5 ± 0.4	NS	NS	NS
Mean inspiratory rate (MIF) (ml/s)	4.5 ± 0.3	5.4 ± 0.2	NS	4.2 ± 0.2	4.5 ± 0.2	NS	NS	<0.05
Mean expiratory rate (MEF) (ml/s)	2.7 ± 0.08	2.6 ± 0.2	NS	2.2 ± 0.1	2.1 ± 0.2	NS	<0.01	<0.05
Activity								
Respiratory rate (f) (1/min)	473.8 ± 6.9	506.5 ± 2.7	NS	472.6 ± 6.6	512.6 ± 11.0	<0.02	NS	NS
Tidal volume (TV) (ml)	0.31 ± 0.01	0.29 ± 0.02	NS	0.26 ± 0.01	0.24 ± 0.01	NS	<0.02	<0.05
Specific tidal volume (sTV) (μl/g)	9.7 ± 0.8	12.1 ± 0.7	NS	8.6 ± 0.4	10.5 ± 0.8	NS	NS	NS
Minute ventilation (MV) (ml/min)	144.8 ± 5.2	147.7 ± 12.3	NS	119.5 ± 3.5	123.1 ± 7.3	NS	<0.01	NS
Specific minute ventilation (sMV) (ml/g)	4.5 ± 0.3	6.1 ± 0.5	<0.05	4.0 ± 0.2	5.3 ± 0.5	NS	NS	NS
Inspiratory time (Ti) (ms)	48.1 ± 0.9	43.9 ± 1.1	<0.02	45.3 ± 0.9	41.9 ± 0.4	<0.01	NS	NS
Expiratory time (Te) (ms)	78.6 ± 2.4	75.0 ± 3.4	NS	81.7 ± 1.1	75.4 ± 2.4	NS	NS	NS
Fraction of respiration (Ti/TT)	0.38 ± 0.01	0.37 ± 0.01	NS	0.36 ± 0.01	0.36 ± 0.01	NS	NS	NS
Peak inspiratory rate (PIF) (ml/s)	10.8 ± 0.7	11.4 ± 0.8	NS	10.0 ± 0.4	10.1 ± 0.5	NS	NS	NS
Peak expiratory rate (PEF) (ml/s)	9.4 ± 0.4	9.0 ± 1.1	NS	8.1 ± 0.6	7.5 ± 0.5	NS	NS	NS
Mean inspiratory rate (MIF) (ml/s)	6.5 ± 0.4	6.7 ± 0.4	NS	5.6 ± 0.2	5.8 ± 0.3	NS	NS	NS
Mean expiratory rate (MEF) (ml/s)	3.9 ± 0.1	3.9 ± 0.4	NS	3.1 ± 0.1	3.2 ± 0.2	NS	<0.001	NS

[a] Data are from 14-week-old mice and are shown as means ± SEM. NS, not significant.

staining. Likewise, in situ hybridization for *dkk3* confirmed downregulation of expression in mutant mice (see below). *dkk3*$^{-/-}$ mice had normal size and body weight and overall were in good general health (well-groomed coat and normal body posture and righting reflex; not shown). A gross neurological examination of animals revealed no sign of modified sensory functions, as assessed by basic tests of vision, audition, olfaction, and touch sensitivity. No enhanced tumorigenesis or major reduction in life span was observed.

Phenotypic analysis in the GMC. *dkk3*$^{-/-}$ mice were subjected to phenotypic analysis in the GMC, an open access platform for standardized phenotyping (11). Overall, several hundred parameters, including analysis of morphology, behavior, neurology, vision and eye, clinical-chemical parameters, immunological status, nociception, lung function, and organ pathology were assessed. Four main significant differences between *dkk3* mutant mice and their wild-type littermates were observed, as described below.

Behavioral phenotype. A locomotor activity-related phenotype was observed with *dkk3*-deficient female mice (Table 1). *dkk3*$^{-/-}$ females were hyperactive, which was reflected by an increased number of line crossings, increased distance moved, and an increased number of turns made within the observation period. Corresponding effects in males just missed statistical significance. *dkk3*$^{-/-}$ females also reached a higher maximum velocity while exploring the arena, and additionally there was a

TABLE 4. Results of GMC immunology screen[a]

Parameter	Control (A)			Mutant (B)			A~B (*P* value)	
	Male ($n = 13$)	Female ($n = 14$)	*P* value	Male ($n = 12$)	Female ($n = 15$)	*P* value	Male	Female
$CD19^+$	39.6 ± 3.4	45.0 ± 2.7	NS	46.4 ± 3.0	44.5 ± 1.0	NS	NS	NS
$CD19^+$ $CD5^-$	97.8 ± 0.2	94.1 ± 0.4	<0.001	98.0 ± 0.3	94.0 ± 0.5	<0.001	NS	NS
$CD19^+$ $CD5^+$	2.2 ± 0.2	5.6 ± 0.3	<0.001	2.0 ± 0.3	5.7 ± 0.5	<0.001	NS	NS
$CD3^+$	21.8 ± 2.3	29.9 ± 2.7	<0.05	21.7 ± 1.2	30.4 ± 1.6	<0.01	NS	NS
γ/δ TCR^+	0.4 ± 0.1	0.2 ± 0.03	<0.001	0.3 ± 0.02	0.2 ± 0.04	NS	NS	NS
$Gr\text{-}1^+$	39.9 ± 5.3	19.6 ± 1.7	<0.01	33.5 ± 5.4	18.8 ± 1.1	NS	NS	NS
$CD49b^+$	26.8 ± 2.4	27.2 ± 2.6	NS	23.1 ± 1.9	34.2 ± 2.1	<0.001	NS	<0.05
$CD4^+$	11.7 ± 1.1	17.1 ± 1.2	<0.01	11.7 ± 1.0	17.8 ± 1.3	<0.01	NS	NS
$CD8\beta^+$	8.3 ± 0.8	11.4 ± 0.5	<0.01	8.2 ± 0.7	12.8 ± 0.7	<0.001	NS	NS
IgG1	113.5 ± 24.3	315.4 ± 20.9	<0.001	208.7 ± 45.5	517.3	NS	NS	NS
IgG2a	178.8 ± 18.8	154.8 ± 8.3	NS	224.8 ± 24.8	158.0 ± 6.1	<0.01	NS	NS
IgG2b	286.9 ± 60.2	NA	NA	280.2 ± 68.4	NA	NA	NS	NA
IgG3	293.3 ± 79.0	1199.3 ± 266.9	<0.001	268.7 ± 57.0	1159.9 ± 354.3	<0.001	NS	NS
IgM	306.6 ± 40.9	388 ± 58.8	NS	604.1 ± 95.4	717.9 ± 103.7	NS	<0.01	<0.01
IgA	98.8 ± 16.7	178.1 ± 36.6	NS	134.1 ± 16.3	132.7 ± 17.0	NS	NS	NS

[a] Data are from 12-week-old mice, presented as means ± SEM. NS, not significant; NA, not analyzed.

TABLE 5. *dkk3* and *p29* mRNA levels in mouse brain at postnatal day 11[a]

Region	Mouse *dkk3*		Rat *p29*	
	WT	*dkk3*$^{-/-}$	WT	*dkk3*$^{-/-}$
CA1-4	++++	++	++++	+
DG	+	+	+	+
Cingulate Cx	+++	+	+++	+
Retrosplenial Cx	++++	++	++++	+
Piriform Cx	+++	+	+++	+
Smt Cx I	±	−	−	−
Smt Cx II-III	±	−	−	−
Smt Cx IV-V	+	−	++	+
Smt Cx VI	++	+	++	±*
Lateral ventricles (both sides)	+++	−	++	−
Third ventricle	++++	−	++	−
Circumventricular organs	++++	−	++++	−
Cerebellum egl	−	−	−	−
Cerebellum Mol	−	−	−	−
Purkinje cell layer	++	−	++	−
Cerebellum igl	++	−	++	−
Choroid plexus	+	−	+	−
Leptomeninges	+	±	+	±
Olfact. epithelium	++	−	+	−
Ant. olfact. nucleus	+	−	+	±

[a] Qualitative autoradiographic analysis. The maximum signal is considered as a very high signal (++++) and the rest in proportion to this: high (+++), moderate (++), low (+), either noise or very low labeling (not easy to confirm) (±), no signal (−). Abbreviations: I to VI, layers of the neocortex; CA1-4, Ammon's horn of the hippocampus; Cx, neocortex; DG, dentate gyrus; egl, external granular layer; igl, internal granular layer; Mol, molecular layer; Smt, somatosensorial; * anterior-posterior expression differences; no expression in anterior levels, low in intermediate levels, and higher in sections containing the hippocampus.

trend toward increased mean velocity. This hyperactivity was also reflected in trends toward increased hole exploration, increased rearing on the board, and reduced grooming. There were no specific effects on anxiety-related (board entry) behavior.

Red blood cell phenotype. Red blood cells of *dkk3*$^{-/-}$ mice showed a higher mean corpuscular volume and mean corpuscular hemoglobin (MCH) content but a reduced MCH concentration, compared to their littermate controls, resulting in an elevated hematocrit and total hemoglobin concentration in blood (Table 2).

Lung phenotype. While control and mutant mice breathed at similar respiratory rates, tidal volumes in mutants were smaller than those in control animals, both at rest and during activity (Table 3). As a result, minute ventilation was about 20% lower in mutant mice. Differences were less pronounced when body weight-specific ventilation was considered.

Immunological phenotype. *dkk3*$^{-/-}$ mice showed a two-times-higher IgM level than littermate controls. We also detected a slight, but statistically significant increase in the frequency of natural killer (NK) cells (CD49b^{+}) in *dkk3*$^{-/-}$ females. No significant differences were found with regard to the other cell subsets and immunoglobulins included in the screen (Table 4).

Expression of *dkk3* and *p29* in wild-type and *dkk3* mutant mice. A truncated rat Dkk3 (p29) was implicated as the thyroid hormone binding subunit of D2. To analyze the possibility that *p29* and *dkk3* display distinct expression patterns, e.g., due to alternative promoters, and that *p29* expression may be unaffected in *dkk3* mutants, we first compared the expression pattern of a mouse *dkk3* 5′ probe with the expression pattern

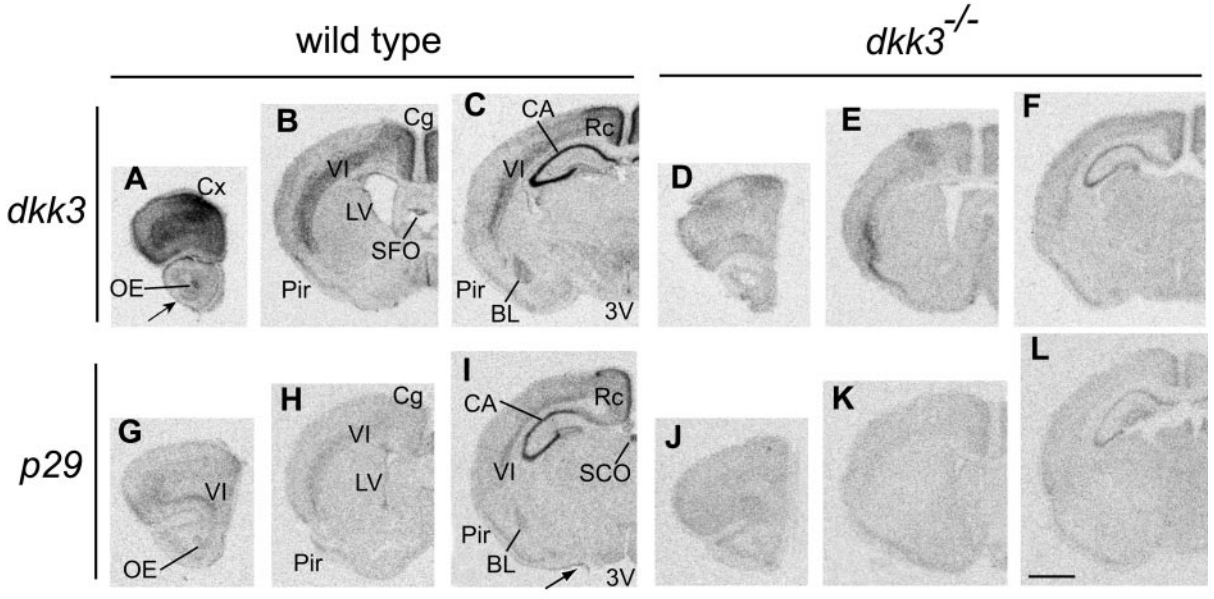

Figure 2

FIG. 2. Comparative regional expression of *dkk3* and *p29* mRNA in wild-type and *dkk3* mutant mice. Three representative autoradiographs of coronal sections organized from anterior to posterior levels are shown. Cx, neocortex; OE, olfactory epithelium; Pir, piriform cortex; VI, layer of the neocortex; Cg, cingulate cortex; LV, lateral ventricle; SFO, subfornical organ; Rc, retrosplenial cortex; CA, Ammon's horn of the hippocampus; BL, basolateral amygdaloid nucleus; 3V, third ventricle; SCO, subcommissural organ. The arrows (A and I) point to the meninges. Scale bar, 150 μm.

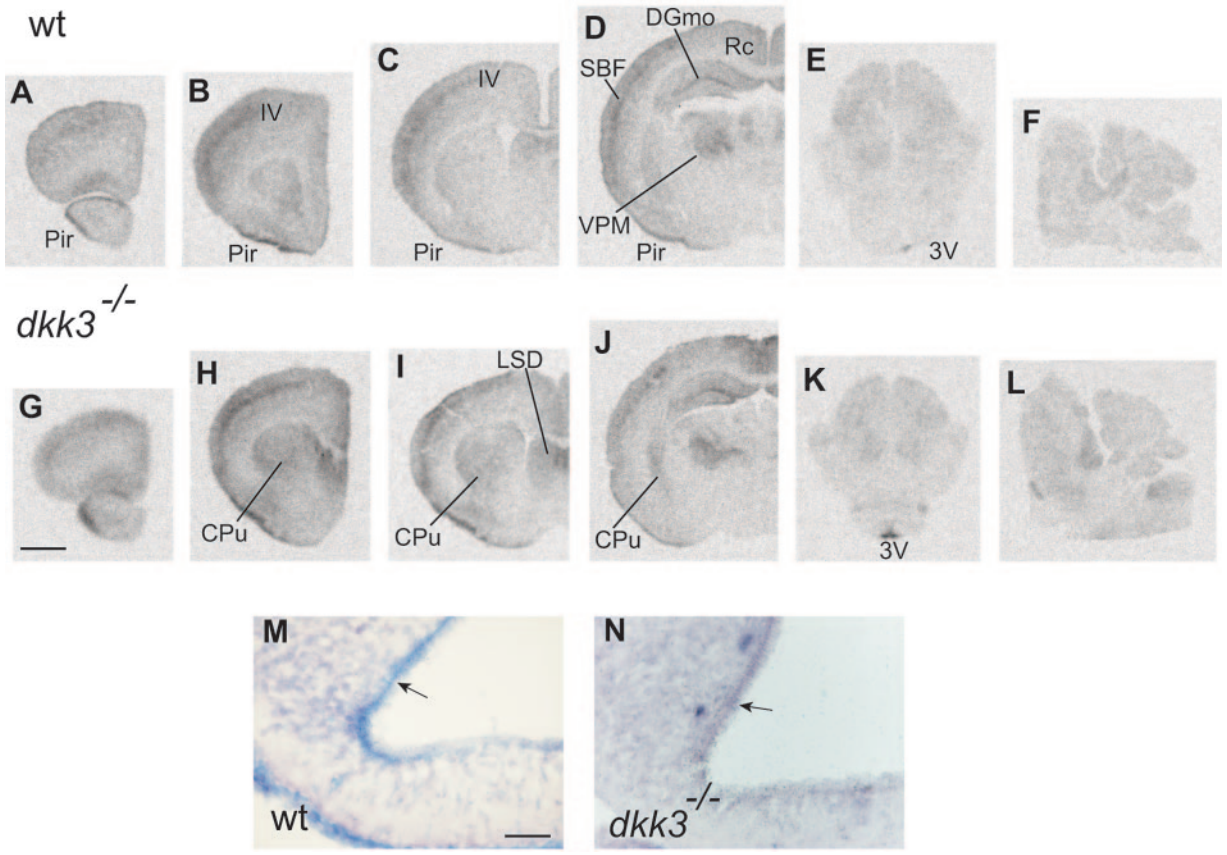

FIG. 3. D2 expression in wild-type and *dkk3* mutant mice. (A to L) Regional expression of *D2* mRNA in wild-type (A to F) and mutant (G to L) mice. Representative coronal sections are organized from anterior to posterior levels. The cerebella were studied in sagittal sections. Pir, piriform cortex; IV, layer of the neocortex; SBF, barrel field of the somatosensory cortex; Rc, retrosplenial cortex; DGmo, molecular layer of the dentate gyrus; VPM, ventral posteromedial thalamic nucleus; 3V, third ventricle; CPu, caudate-putamen; LSD, lateral septal nucleus, dorsal part. Scale bar, 150 μm. (M and N) Micrographs showing the localization of *D2* mRNA in the tanycytes of the third ventricle of wild-type (M) and mutant (N) mice. Arrows point to black silver grains. Scale bar, 50 μm.

representing bona fide rat *p29*. Rat *p29* has 87% similarity to mouse *dkk3* at the nucleotide level, and a *p29* probe can be used for in situ hybridization in mice (34). In wild-type animals, the distribution of the hybridization signal in brain slices obtained with the *p29*- and *dkk3*-specific probes was almost identical, although the *p29* probe gave weaker signals (Table 5), similar to the pattern of the same *p29* probe in rat brain (34). The most prominent signals for *dkk3* and *p29* were observed in the Ammon's horn of the hippocampus; cingulate, retrosplenial, and piriform cortices; and layer VI of the somatosensorial cortex (Fig. 2A to C and G to I). There was also considerable expression in the internal granular layer and Purkinje cell layer of the cerebellum (not shown) and in the olfactory epithelium (Fig. 2A and G). In addition to expression in neuronal cells, *dkk3* was expressed in epithelial cells lining the lateral and third ventricles with a high hybridization signal in tanycytes (Table 5). Other important sites for communication with the cerebrospinal fluid (CSF) such as the choroid plexus and leptomeninges of the blood-cerebrospinal fluid barrier and the circumventricular organs also showed *dkk3* expression. Especially high levels of *dkk3* expression were found in the subfornical and subcommissural organs (Fig. 2B and I).

In *dkk3* mutants, hybridization signals for *dkk3* and *p29* were very weak (Fig. 2D to F and J to L) and limited to the regions of the cerebral cortex, which also had the highest hybridization signal in wild-type mice (Fig. 2D to F).

Taken together, the common expression pattern of mouse *dkk3* and rat *p29*,as well as their common downregulation in *dkk3* mutants, supports the notion that *dkk3* and *p29* represent the same gene under a common promoter, both of which are inactivated in *dkk3* mutants.

Normal D2 expression and activity in *dkk3* mutants. Expression and activity of D2 in brain are homeostatically regulated by thyroid hormone status such that they increase in hypothyroidism and decrease in hyperthyroidism to maintain normal T3 concentrations (14, 27, 54). Therefore, we tested the possibility that *D2* expression was altered in *dkk3* mutant mice. The distribution of *D2* mRNA in the brains of wild-type mice was similar to that in *dkk3* mutants (Fig. 3A to L) and to that previously reported for rats (15). The hybridization signal was mainly localized in tanycytes lining the walls of the third ventricle and astrocytes in several brain regions (Fig. 3). There was only a slightly increased expression in the retrosplenial cortex and tanycytes of the third ventricle in $dkk3^{-/-}$ mice (Fig. 3J and K).

To extend the results described above, D2 enzyme activity in

TABLE 6. *D2* and *D1* activities in several organs of adult WT and *dkk3*$^{-/-}$ mice[a]

Mouse line	Organ			
	BAT D2	Neocortex D2	Cerebellum D2	Rest of brain D2
WT males	21.6 ± 2.4 (6)	30.6 ± 2.6 (7)	20.1 ± 3.6 (8)	18.4 ± 3.9 (5)
dkk3$^{-/-}$ males	30.1 ± 5.3 (6)	32.9 ± 1.1 (5)	30.7 ± 1.6 (7)[b]	15.5 ± 3.4 (3)
WT females	32.0 ± 3.6 (8)[c]	38.6 ± 1.7 (9)[c]	23.8 ± 2.4 (9)	7.9 ± 3.8 (3)[c]
dkk3$^{-/-}$ females	28.5 ± 2.1 (11)	19.6 ± 1.8 (10)[b,c]	20.3 ± 2.5 (12)[c]	7.0 ± 1.4 (4)
	Pituitary D1	Pituitary D2		
WT males	608 ± 99 (7)	315 ± 48 (8)		
dkk3$^{-/-}$ males	366 ± 44 (6)[b]	411 ± 55 (6)		
WT females	391 ± 58 (8)[c]	469 ± 28 (8)[c]		
dkk3$^{-/-}$ females	529 ± 47 (9)	570 ± 45 (12)[c]		
	Liver D1	Kidney D1		
WT males	6.23 ± 0.45 (7)	1.54 ± 0.08 (7)		
dkk3$^{-/-}$ males	4.60 ± 0.26 (5)[b]	1.67 ± 0.25 (7)		
WT females	5.24 ± 0.44 (8)	3.21 ± 0.09 (9)[c]		
dkk3$^{-/-}$ females	5.63 ± 0.40 (11)	3.19 ± 0.15 (10)		

[a] D2 activities were determined using 2 nM T4 as substrate (results are expressed in femtomoles per hour per milligram of protein). For pituitaries D1 and D2, activities were determined by using 2 nM rT3 as substrate (in femtomoles per hour per milligram of protein). D1 activities in liver and kidney were determined by using 400 nM rT3 (picomoles per minute per milligram of protein). Data are means ± SEM. The number of animals used is indicated in parentheses.
[b] $P < 0.05$, *dkk3*$^{-/-}$ versus WT.
[c] $P < 0.05$, males versus females.

different brain regions, in BAT, and pituitaries was determined. If *dkk3* was required for D2 deiodinase activity, a decrease in D2 enzymatic activity in *dkk3* mutants may be expected.

The results are summarized in Table 6. Males and females were analyzed separately, as sex-related differences were observed in some tissues. There were no differences in D2 activity between wild-type and *dkk3* mutant mice, except for a 50% decrease in the neocortex of *dkk3*$^{-/-}$ females and a 50% increase in the cerebellum of *dkk3*$^{-/-}$ males. No differences in *D2* activity were observed in pituitaries. We also analyzed D1 activity, as it may compensate for loss of D2 activity, and generally found no major changes in *dkk3* mutants (Table 6). Only in mutant males was a decrease in D1 activity observed, in pituitary (by 40%) and liver (by 25%). We conclude that D1 and D2 activities are unaffected in most tissues in *dkk3* mutant mice.

***dkk3* mutants are euthyroid.** If a truncated rat Dkk3 (p29) was implicated as the thyroid hormone binding subunit of D2 enzyme, production of T3 should decrease in *dkk3* mutant animals in those tissues in which T3 levels are dependent on the local T3 production via D2, such as brain and BAT (47, 48).

Therefore, T4 and T3 levels were measured in several tissues and in plasma of wild-type and *dkk3* mutant mice (Table 7). No changes were observed in most tissues studied. T3 was decreased in the kidney of *dkk3* mutant males (by 22%). T4 was elevated by 30% in the neocortex of *dkk3* mutant females and T3 (by 28%) in the liver of *dkk3* mutant females. These isolated changes in T4 and T3 concentrations are unlikely to be direct consequences of *dkk3* deletion. We conclude that no major changes in T3 concentrations are found and that most tissues of *dkk3* mutant mice remain euthyroid.

Conclusions. Our data indicate that *dkk3* is not essential for embryogenesis and viability, and they neither support a role in thyroid hormone metabolism nor indicate that p29 is a naturally occurring variant of physiological relevance.

Initial phenotyping reveals abnormalities in hematological and immunological parameters, lung ventilation, and behavior. In particular, the observed hyperactivity phenotype may be

TABLE 7. T4 and T3 concentrations in plasma and several organs of adult WT and *dkk3*$^{-/-}$ mice[a]

Concn (ng/g)	Organ						
	Plasma	BAT	Neocortex	Cerebellum	Rest of brain	Liver	Kidney
T4							
WT males	43.0 ± 2.7 (7)	6.33 ± 0.36 (8)	2.35 ± 0.15 (8)	18.75 ± 0.64 (6)	3.18 ± 0.16 (6)	31.5 ± 2.66 (6)	20.42 ± 1.11 (7)
dkk3$^{-/-}$ males	59.0 ± 7.9 (7)	6.04 ± 0.36 (6)	2.49 ± 0.32 (7)	15.85 ± 2.70 (6)	3.05 ± 0.30 (6)	28.17 ± 1.61 (7)	20.01 ± 3.41 (7)
WT females	46.8 ± 5.7 (6)	9.6 ± 0.66 (9)[c]	2.50 ± 0.12 (8)	14.51 ± 1.87 (9)	3.75 ± 0.35 (9)	28.7 ± 1.33 (8)	21.86 ± 1.16 (7)
dkk3$^{-/-}$ females	41.9 ± 5.8 (11)[c]	9.12 ± 0.60 (11)[c]	3.25 ± 0.17 (11)[b,c]	18.68 ± 2.09 (10)	3.35 ± 0.11 (11)	29.5 ± 1.13 (11)	22.23 ± 1.54 (11)
T3							
WT males	0.23 ± 0.02 (7)	2.00 ± 0.14 (8)	1.35 ± 0.21 (3)	2.74 ± 0.34 (7)	1.65 ± 0.07 (8)	2.75 ± 0.23 (6)	3.25 ± 0.11 (7)
dkk3$^{-/-}$ males	0.28 ± 0.03 (7)	1.71 ± 0.08 (6)	1.67 ± 0.18 (7)	2.66 ± 0.66 (6)	1.68 ± 0.10 (6)	3.23 ± 0.18 (7)	2.52 ± 0.24 (7)[b,c]
WT females	0.25 ± 0.01 (8)	2.97 ± 0.28 (9)[c]	1.34 ± 0.08 (8)	2.09 ± 0.18 (7)	1.82 ± 0.11 (9)	2.58 ± 0.15 (8)	3.15 ± 0.23 (9)
dkk3$^{-/-}$ females	0.24 ± 0.01 (11)	2.73 ± 0.18 (12)[c]	1.38 ± 0.10 (12)	2.99 ± 0.28 (8)	2.02 ± 0.12 (11)[c]	3.32 ± 0.23 (10)[b]	3.14 ± 0.13 (11)

[a] Data are means ± SEM. The number of animals used is indicated in parentheses.
[b] $P < 0.05$, *dkk3*$^{-/-}$ versus WT.
[c] $P < 0.05$, males versus females.

correlated with the expression of *dkk3* in dopaminergic neurons, abnormalities of which have been associated with alterations in locomotor activity. Recombinant Dkk3 promotes differentiation of dopaminergic neurons from undifferentiated precursors (E. Arenas, unpublished results), also hinting at a role for *dkk3* in this process.

Due to their distinct functions, a compensation of *dkk3* deficiency by other *dkk* genes appears unlikely; indeed, *dkk1*/*dkk3* double-mutant mice do not show any synthetic phenotypes (S. Pinho and C. Niehrs, unpublished data). However, combined inactivation of *dkk3* and the unique *dkk3*-related gene *soggy* (24) may reveal roles masked by redundancy.

ACKNOWLEDGMENTS

We thank Sonia Pinho, Dana Hoppe, Socorro Duran, Maria Jesus Presas, Elena Fernandez-Duran, Maria Asuncion Navarro, and Marina Sanz-Sancristobal for excellent technical assistance and the screeners of the German Mouse Clinic for phenotypical analysis of the mice.

This work was supported by the DFG (SFB 488 A1), grants SAF2001-2243 and FIS RCMN 03/08 (M.-J.O.), BFI2001-2412 and BFU2004-05944 (A.G-F.), NGFN 01GR0430, and 01GR0434, 01GR0458, and 01GR0103 (GMC).

REFERENCES

1. **Bafico, A., G. Liu, A. Yaniv, A. Gazit, and S. A. Aaronson.** 2001. Novel mechanism of Wnt signalling inhibition mediated by Dickkopf-1 interaction with LRP6/Arrow. Nat. Cell Biol. **3:**683–686.
2. **Bernal, J.** 2002. Action of thyroid hormone in brain. J. Endocrinol. Investig. **25:**268–288.
3. **Bernal, J., and A. Guadaño-Ferraz.** 2002. Analysis of thyroid hormone-dependent genes in the brain by in situ hybridization. Methods Mol. Biol. **202:**71–90.
4. **Bianco, A. C., D. Salvatore, B. Gereben, M. J. Berry, and P. R. Larsen.** 2002. Biochemistry, cellular and molecular biology, and physiological roles of the iodothyronine selenodeiodinases. Endocr. Rev. **23:**38–89.
5. **Chapman, S. C., R. Brown, L. Lees, G. C. Schoenwolf, and A. Lumsden.** 2004. Expression analysis of chick Wnt and frizzled genes and selected inhibitors in early chick patterning. Dev. Dyn. **229:**668–676.
6. **del Barco Barrantes, I., G. Davidson, H. J. Gröne, H. Westphal, and C. Niehrs.** 2003. Dkk1 and noggin cooperate in mammalian head induction. Genes Dev. **17:**2239–2344.
7. **Diep, D. B., N. Hoen, M. Backman, O. Machon, and S. Krauss.** 2004. Characterisation of the Wnt antagonists and their response to conditionally activated Wnt signalling in the developing mouse forebrain. Brain Res. Dev. Brain Res. **153:**261–270.
8. **Drorbaugh, J. E., and W. O. Fenn.** 1955. A barometric method for measuring ventilation in newborn infants. Pediatrics **16:**81–87.
9. **Fedders, H., R. Augustin, and T. C. Bosch.** 2004. A Dickkopf-3-related gene is expressed in differentiating nematocytes in the basal metazoan Hydra. Dev. Genes Evol. **214:**72–80.
10. **Fjeld, K., P. Kettunen, T. Furmanek, I. H. Kvinnsland, and K. Luukko.** 2005. Dynamic expression of Wnt signaling-related Dickkopf1, -2, and -3 mRNAs in the developing mouse tooth. Dev. Dyn. **233:**161–166.
11. **Gailus-Durner, V., H. Fuchs, L. Becker, I. Bolle, M. Brielmeier, J. Calzada-Wack, R. Elvert, N. Ehrhardt, C. Dalke, T. J. Franz, E. Grundner-Culemann, S. Hammelbacher, S. M. Holter, G. Holzlwimmer, M. Horsch, A. Javaheri, S. V. Kalaydjiev, M. Klempt, E. Kling, S. Kunder, C. Lengger, T. Lisse, T. Mijalski, B. Naton, V. Pedersen, C. Prehn, G. Przemeck, I. Racz, C. Reinhard, P. Reitmeir, I. Schneider, A. Schrewe, R. Steinkamp, C. Zybill, J. Adamski, J. Beckers, H. Behrendt, J. Favor, J. Graw, G. Heldmaier, H. Hofler, B. Ivandic, H. Katus, P. Kirchhof, M. Klingenspor, T. Klopstock, A. Lengeling, W. Muller, F. Ohl, M. Ollert, L. Quintanilla-Martinez, J. Schmidt, H. Schulz, E. Wolf, W. Wurst, A. Zimmer, D. H. Busch, and M. H. de Angelis.** 2005. Introducing the German Mouse Clinic: open access platform for standardized phenotyping. Nat. Methods **2:**403–404.
12. **Glinka, A., W. Wu, H. Delius, A. P. Monaghan, C. Blumenstock, and C. Niehrs.** 1998. Dickkopf-1 is a member of a new family of secreted proteins and functions in head induction. Nature **391:**357–362.
13. **Grotewold, L., T. Theil, and U. Rüther.** 1999. Expression pattern of dkk-1 during mouse limb development. Mech. Dev. **89:**151–153.
14. **Guadaño-Ferraz, A., M. J. Escamez, E. Rausell, and J. Bernal.** 1999. Expression of type 2 iodothyronine deiodinase in hypothyroid rat brain indicates an important role of thyroid hormone in the development of specific primary sensory systems. J. Neurosci. **19:**3430–3439.
15. **Guadaño-Ferraz, A., M. J. Obregon, D. L. St. Germain, and J. Bernal.** 1997. The type 2 iodothyronine deiodinase is expressed primarily in glial cells in the neonatal rat brain. Proc. Natl. Acad. Sci. USA **94:**10391–10396.
16. **Guder, C., T. Nacak, S. Pinho, E. Hobmayer, C. Niehrs, and T. Holstein.** An ancient Wnt-Dickkopf antagonism in hydra. Development, in press.
17. **Hackam, A. S., R. Strom, D. Liu, J. Qian, C. Wang, D. Otteson, T. Gunatilaka, R. H. Farkas, I. Chowers, M. Kageyama, T. Leveillard, J. A. Sahel, P. A. Campochiaro, G. Parmigiani, and D. J. Zack.** 2004. Identification of gene expression changes associated with the progression of retinal degeneration in the rd1 mouse. Investig. Ophthalmol. Vis. Sci. **45:**2929–2942.
18. **Hashimoto, H., M. Itoh, Y. Yamanaka, S. Yamashita, T. Shimizu, L. Solnica-Krezel, M. Hibi, and T. Hirano.** 2000. Zebrafish Dkk1 functions in forebrain specification and axial mesendoderm formation. Dev. Biol. **217:**138–152.
19. **Hsieh, S. Y., P. S. Hsieh, C. T. Chiu, and W. Y. Chen.** 2004. Dickkopf-3/REIC functions as a suppressor gene of tumor growth. Oncogene **23:**9183–9189.
20. **Idkowiak, J., G. Weisheit, J. Plitzner, and C. Viebahn.** 2004. Hypoblast controls mesoderm generation and axial patterning in the gastrulating rabbit embryo. Dev. Genes Evol. **214:**591–605.
21. **Kaplan, M. M., and K. A. Yaskoski.** 1981. Maturational patterns of iodothyronine phenolic and tyrosyl ring deiodinase activities in rat cerebrum, cerebellum, and hypothalamus. J. Clin. Investig. **67:**1208–1214.
22. **Kazanskaya, O., A. Glinka, and C. Niehrs.** 2000. The role of Xenopus dickkopf1 in prechordal plate specification and neural patterning. Development **127:**4981–4992.
23. **Kobayashi, K., M. Ouchida, T. Tsuji, H. Hanafusa, M. Miyazaki, M. Namba, N. Shimizu, and K. Shimizu.** 2002. Reduced expression of the REIC/Dkk-3 gene by promoter-hypermethylation in human tumor cells. Gene **282:**151–158.
24. **Krupnik, V. E., J. D. Sharp, C. Jiang, K. Robison, T. W. Chickering, L. Amaravadi, D. E. Brown, D. Guyot, G. Mays, K. Leiby, B. Chang, T. Duong, A. D. Goodearl, D. P. Gearing, S. Y. Sokol, and S. A. McCarthy.** 1999. Functional and structural diversity of the human Dickkopf gene family. Gene **238:**301–313.
25. **Kurose, K., M. Sakaguchi, Y. Nasu, S. Ebara, H. Kaku, R. Kariyama, Y. Arao, M. Miyazaki, T. Tsushima, M. Namba, H. Kumon, and N. H. Huh.** 2004. Decreased expression of REIC/Dkk-3 in human renal clear cell carcinoma. J. Urol. **171:**1314–1318.
26. **Leonard, D. M., S. J. Stachelek, M. Safran, A. P. Farwell, T. F. Kowalik, and J. L. Leonard.** 2000. Cloning, expression, and functional characterization of the substrate binding subunit of rat type II iodothyronine 5′-deiodinase. J. Biol. Chem. **275:**25194–25201.
27. **Leonard, J. L., M. M. Kaplan, T. J. Visser, J. E. Silva, and P. R. Larsen.** 1981. Cerebral cortex responds rapidly to thyroid hormones. Science **214:**571–573.
28. **Li, X., P. Liu, W. Liu, P. Maye, J. Zhang, Y. Zhang, M. Hurley, C. Guo, A. Boskey, L. Sun, S. E. Harris, D. W. Rowe, H. Z. Ke, and D. Wu.** 2005. Dkk2 has a role in terminal osteoblast differentiation and mineralized matrix formation. Nat. Genet. **37:**945–952.
29. **Mao, B., and C. Niehrs.** 2003. Kremen2 modulates Dickkopf2 activity during Wnt/LRP6 signaling. Gene **302:**179–183.
30. **Mao, B., W. Wu, G. Davidson, J. Marhold, M. Li, B. Mechler, H. Delius, D. Hoppe, P. Stannek, C. Walter, A. Glinka, and C. Niehrs.** 2002. Kremens are novel Dickkopf receptors that regulate Wnt/beta-catenin signalling. Nature **417:**664–667.
31. **Mao, B., W. Wu, Y. Li, D. Hoppe, P. Stannek, A. Glinka, and C. Niehrs.** 2001. LDL-receptor-related protein 6 is a receptor for Dickkopf proteins. Nature **411:**321–325.
32. **Mao, J., J. Wang, B. Liu, W. Pan, G. H. Far III, C. Flynn, H. Yuan, S. Takada, D. Kimelman, L. Li, and D. Wu.** 2001. Low-density lipoprotein receptor-related protein-5 binds to Axin and regulates the canonical Wnt signaling pathway. Mol. Cell **7:**801–809.
33. **Monaghan, A. P., P. Kioschis, W. Wu, A. Zuniga, D. Bock, A. Poustka, H. Delius, and C. Niehrs.** 1999. Dickkopf genes are co-ordinately expressed in mesodermal lineages. Mech. Dev. **87:**45–56.
34. **Montero-Pedrazuela, A., J. Bernal, and A. Guadaño-Ferraz.** 2003. Divergent expression of type 2 deiodinase and the putative thyroxine-binding protein p29, in rat brain, suggests that they are functionally unrelated proteins. Endocrinology **144:**1045–1052.
35. **Morreale de Escobar, G., R. Pastor, M. J. Obregon, and F. Escobar del Rey.** 1985. Effects of maternal hypothyroidism on the weight and thyroid hormone content of rat embryonic tissues, before and after onset of fetal thyroid function. Endocrinology **117:**1890–1900.
36. **Mukhopadhyay, M., S. Shtrom, C. Rodriguez-Esteban, L. Chen, T. Tsukui, L. Gomer, D. W. Dorward, A. Glinka, A. Grinberg, S. P. Huang, C. Niehrs, J. C. Belmonte, and H. Westphal.** 2001. Dickkopf1 is required for embryonic head induction and limb morphogenesis in the mouse. Dev. Cell **1:**423–434.
37. **Nozaki, I., T. Tsuji, O. Iijima, Y. Ohmura, A. Andou, M. Miyazaki, N. Shimizu, and M. Namba.** 2001. Reduced expression of REIC/Dkk-3 gene in non-small cell lung cancer. Int. J. Oncol. **19:**117–121.
38. **Obregon, M. J., J. Mallol, F. Escobar del Rey, and G. Morreale de Escobar.** 1981. Presence of L-thyroxine and 3,5,3′-triiodo-L-thyronine in tissues from thyroidectomized rats. Endocrinology **109:**908–913.

39. **Obregon, M. J., C. Ruiz de Ona, A. Hernandez, R. Calvo, F. Escobar del Rey, and G. Morreale de Escobar.** 1989. Thyroid hormones and 5′-deiodinase in rat brown adipose tissue during fetal life. Am. J. Physiol. **257:**E625–E631.
40. **Ohl, F., F. Holsboer, and R. Landgraf.** 2001. The modified hole board as a differential screen for behavior in rodents. Behav. Res. Methods Instrum. Comput. **33:**392–397.
41. **Ohl, F., I. Sillaber, E. Binder, M. E. Keck, and F. Holsboer.** 2001. Differential analysis of behavior and diazepam-induced alterations in C57BL/6N and BALB/c mice using the modified hole board test. J. Psychiatr. Res. **35:**147–154.
42. **Paxinos, G., and K. B. J. Franklin.** 2001. The mouse brain in stereotaxic coordinates. Academic Press, London, United Kingdom.
43. **Roman-Gomez, J., A. Jimenez-Velasco, X. Agirre, J. A. Castillejo, G. Navarro, M. Barrios, E. J. Andreu, F. Prosper, A. Heiniger, and A. Torres.** 2004. Transcriptional silencing of the Dickkopfs-3 (Dkk-3) gene by CpG hypermethylation in acute lymphoblastic leukaemia. Br. J. Cancer **91:**707–713.
44. **Ruiz de Ona, C., G. Morreale de Escobar, R. Calvo, F. Escobar del Rey, and M. J. Obregon.** 1991. Thyroid hormones and 5′-deiodinase in the rat fetus late in gestation: effects of maternal hypothyroidism. Endocrinology **128:**422–432.
45. **Semenov, M. V., K. Tamai, B. K. Brott, M. Kuhl, S. Sokol, and X. He.** 2001. Head inducer Dickkopf-1 is a ligand for Wnt coreceptor LRP6. Curr. Biol. **11:**951–961.
46. **Shinya, M., C. Eschbach, M. Clark, H. Lehrach, and M. Furutani-Seiki.** 2000. Zebrafish Dkk1, induced by the pre-MBT Wnt signaling, is secreted from the prechordal plate and patterns the anterior neural plate. Mech. Dev. **98:**3–17.
47. **Silva, J. E., and P. R. Larsen.** 1985. Potential of brown adipose tissue type II thyroxine 5′-deiodinase as a local and systemic source of triiodothyronine in rats. J. Clin. Investig. **76:**2296–2305.
48. **Silva, J. E., and P. S. Matthews.** 1984. Production rates and turnover of triiodothyronine in rat-developing cerebral cortex and cerebellum. Responses to hypothyroidism. J. Clin. Investig. **74:**1035–1049.
49. **Snedecor, G. W., and W. G. Cochran.** 1980. Statistical Methods, 7th ed. Iowa State University Press, Ames, Iowa.
50. **Suwa, T., M. Chen, C. L. Hawks, and P. J. Hornsby.** 2003. Zonal expression of dickkopf-3 and components of the Wnt signalling pathways in the human adrenal cortex. J. Endocrinol. **178:**149–158.
51. **Tankersley, C. G., R. S. Fitzgerald, R. C. Levitt, W. A. Mitzner, S. L. Ewart, and S. R. Kleeberger.** 1997. Genetic control of differential baseline breathing pattern. J Appl. Physiol. **82:**874–881.
52. **Tsuji, T., M. Miyazaki, M. Sakaguchi, Y. Inoue, and M. Namba.** 2000. A REIC gene shows down-regulation in human immortalized cells and human tumor-derived cell lines. Biochem. Biophys. Res. Commun. **268:**20–24.
53. **Tsuji, T., I. Nozaki, M. Miyazaki, M. Sakaguchi, H. Pu, Y. Hamazaki, O. Iijima, and M. Namba.** 2001. Antiproliferative activity of REIC/Dkk-3 and its significant down-regulation in non-small-cell lung carcinomas. Biochem. Biophys. Res. Commun. **289:**257–263.
54. **Tu, H. M., S. W. Kim, D. Salvatore, T. Bartha, G. Legradi, P. R. Larsen, and R. M. Lechan.** 1997. Regional distribution of type 2 thyroxine deiodinase messenger ribonucleic acid in rat hypothalamus and pituitary and its regulation by thyroid hormone. Endocrinology **138:**3359–3368.
55. **Wu, W., A. Glinka, H. Delius, and C. Niehrs.** 2000. Mutual antagonism between dickkopf1 and -2 regulates Wnt/beta-catenin signalling. Curr. Biol. **10:**1611–1614.
56. **Yamaguchi, Y., S. Itami, H. Watabe, K. Yasumoto, Z. A. Abdel-Malek, T. Kubo, F. Rouzaud, A. Tanemura, K. Yoshikawa, and V. J. Hearing.** 2004. Mesenchymal-epithelial interactions in the skin: increased expression of dickkopf1 by palmoplantar fibroblasts inhibits melanocyte growth and differentiation. J. Cell Biol. **165:**275–285.